Role of Purged Air On Synthesis of Mesoporous NiO/C Composite And Its Application On Waste Water Treatment

Saravanakumar Ramalingam
GCT: Government College of Technology
Muthukumaran Karpagasundaram
GCT: Government College of Technology
Sivasankari Chandrasekaran
GCT: Government College of Technology
Sathiyapriya Narayanan
NIET: Nehru Institute of Engineering and Technology
Kathiresan Sakthipandi (sakthipandi@gmail.com)
SRM TRP Engineering College https://orcid.org/0000-0003-3126-0991

Research Article

Keywords: Role of dissolved gases, NiO/Carbon, Carbon composite, Pb(II) ion removal, Heavy metal ions, adsorption

Posted Date: September 21st, 2021

DOI: https://doi.org/10.21203/rs.3.rs-667663/v1

Role of purged air on synthesis of mesoporous NiO/C composite and its application on waste water treatment

Saravanakumar Ramalingam[1]*, Muthukumaran Karpagasundaram[1], Sivasankari Chandrasekaran[1] and Sathiyapriya Narayanan[2], Kathiresan Sakthipandi[3]*

[1]Department of Chemistry, Government College of Technology, Coimbatore, Tamil Nadu641013, India

[2]Department of Physics, Nehru Institute of Engineering and Technology, Coimbatore 641 105, India

[3]Department of Physics, SRM TRP Engineering College, Tiruchirappalli 621 105, Tamil Nadu, India

Abstract

Two different methods were employed to synthesis NiO/C composite from agricultural waste. The mesoporous composite was successfully synthesized via a novel precipitation method in the presence of dissolved gases. The morphology of the composites were differentiated by characterisation techniques such asx-ray Diffraction (XRD), the point of zero charge (pH_{pzc}), field emission scanning electron microscope (FESEM), Fourier transform infrared spectroscopy (FTIR), energy dispersive x-ray analysis (EDAX) and vibrating sample magnetometer (VSM). Then, the mechanism of synthesis was elucidated using the above experimental characterisation data. FESEM and EDAX report of $Ni(OH)_2$-carbon composite clearly showed the role of dissolved gases on synthesis. Both the composites were subjected as the adsorbent to eliminate/remove the toxic Pb(II) ions from the wastewater. Batch adsorption experiments were carried out to compare the Pb(II) ions removal capability of both the composite materials. The parameters such as the effect of pH, the dosage of the adsorbents and initial concentration were studied. At the optimized conditions, isotherm studies for each of the adsorbents were also carried out. The isotherm results revealed that the maximum removal capacity q_e (mg/g) was 30.78 for PJNC and 43.48 for PJGNC. The VSM analysis confirmed that both the adsorbents were soft magnetic materials. Hence, they could be competently separated from salted/treated water using the magnetic field.

Keywords: Role of dissolved gases; NiO/Carbon; Carbon composite; Pb(II) ion removal; Heavy metal ions; adsorption;

*Corresponding author: saravanan.chem111@gmail.com; sakthipandi@gmail.com

Mobile number: +91 9500477458

1. Introduction

The earth is surrounded by three-fourth of water. Despite this statistical fact, there is more demand for potable water due to urbanization and industrialization (Luzardo et al. 2017). The heavy metal ions such as Pb(II), Cu(II), Hg(II), Cd(II) and Cr(IV) in aquatic streams credibly threaten the environment directly (Sdiri and Higashi 2013; Zhang et al. 2018). Research interests on the potential removal/subtraction of toxic

metal ions from the wastewater could be carried out by various methods like chemical precipitation, coagulation, electro floatation, ion exchange, adsorption, photo-degradation and membrane filtration (Hua et al. 2012; Shaheen et al. 2018; Wan Ngah and Hanafiah 2008). Among these previous methods, adsorption technique is more efficient, cost- effective and it is also an eco-friendly process. The economic adsorption process could be appropriately determined by the proper selection of the cheapest and the most effective adsorbent. Activated carbon is the most commonly used absorbent today as it is the most economical and efficient.The present investigation focuses on the utility of the bio-waste material and it is expected to perform better than the commercial activated carbon (Sud et al. 2008; Wan Ngah and Hanafiah 2008). In this study, carbon has been derived from *prosopis juliflora* wood (PJ) which is invasive to the environment. *prosopisjuli flora* is usually found in abundance in the arid and semi-arid continents (El-Keblawy and Abdelfatah 2014; Shackleton et.al 2015; Zachariades et al. 2011).

In the recent times, researchers have paid attention to convert the nano metal oxides such as ferric oxides, aluminium oxides, manganese oxides, magnesium oxides, cerium oxides and titanium oxides as an efficient adsorbent, since they have the large surface area and high activities with magnetic regeneration property (Hua et al. 2012; Zachariades et al. 2011). Metal oxides are more effective, but they are not cost-effective. Latest studies reveal that metal oxide/carbon composites play a key role in high vital power devices, electrochemical capacitors, catalysts and adsorbents (Fu et al. 2019; Modwi, et al. 2017; Wu and Hsieh 2008) because the metal oxide/ carbon composites are efficient and cost-effective. Hence many efforts have been attempted to synthesize the efficient carbon composite. The features of the composite have been determined by the method of synthesis (Hale 1976; Zachariades et al. 2011). In this study, NiO/carbon composite has been synthesized by precipitation method using sodium hydroxide and nickel nitrate. In another way,the same precipitation is carried out with air as predecessor. The composites which prepared by aforementioned methods have been differentiated by characterisation techniques such as the point of zero charge (pHpzc),x-ray Diffraction (XRD), Fourier transform infrared spectroscopy (FTIR), energy dispersive x-ray analysis (EDAX), field emission scanning electron microscope (FESEM) and vibrating sample magnetometer (VSM). The mechanism of synthesis has been discussed and explored by using the above mentioned experimental characterisation data. Then, those composites were subjected to purify the wastewater to determine the efficiency variance. This comfortable/contented discusses the activity of two different NiO/C composites efficiency in the removal/deduction of Pb (II) ions from aqueous solution.

2. Material and methods

63 **2. 1. Materials**

64 The analytical grade (AR) reagents like nickel nitrate ($NiNO_3$),lead nitrate [$Pb(NO_3)_2$] and sodium
65 hydroxide (NaOH)were purchased from Merck Chemicals, Mumbai, India. The carbon was derived from
66 biological invasive matter (*prosopis juliflora wood).*

67 **2.2. Synthesis of *prosopis juliflora* Carbon**

68 The *prosopis juliflora*wood (PJ) parts were collected from places in and around Coimbatore
69 (11.0168° N, 76.9558° E), India. The wood PJ was wrecked and broken into comparablesimilar sizes (2-3
70 cm) and later washedgently by using double distilled water. The PJ wood pieces were taken in the muffle
71 furnace and exposed to pyrolysis with the slow heating rate (5 K/min)(Estela et.al 2018). It was kept in the
72 furnace up to 673 K in order toget/acquire a high yield of carbon (Selvaraju et.al 2018). The prepared carbon
73 (named as *prosopis juliflora* carbon; PJC) from *prosopis juliflora*was washed thoroughly using double
74 distilled water to remove the ash and some dissolved matter. Then, it was dried and cooled to atmospheric
75 temperature. The PJC which was obtained from the above process was crushed and converted to composite
76 with NiO by two different precipitation methods.

77 **2.3 Synthesis of NiO/C composites**

78 4.6 g of PJC was taken into the clean beaker along with 400 mL of distilled water. Around half an
79 hour, that heterogeneous solution was constantly air purged with a flow rate of 2×10^{-2} m^3/ hr. Then 50 mL of
80 1 M $NiNO_3$ was added to the above and the purging process continued about 30 minutes for even dispersion.
81 To this mixture, 50 mL of 2.0 M NaOHat periodic intervals was added gradually. It resulted in green
82 coloured$Ni(OH)_2$ precipitate on the surface of the carbon. That mixture was kept for a whole day for the
83 settlement of $Ni(OH)_2$/PJC composite (PJGNH) at the bottom. The filtrate was decanted and the residue was
84 washed with double distilled water to attain neutral pH. Then, the final product was kept in a muffle furnace
85 and heated for half an hour upto 250 °C to get a black colour *prosopis juliflora* shell consequential
86 nanocomposite NiO/PJC (PJGNC) (Xing et.al 2004 ; Yuan et.al 2005). The synthesis procedure/process is
87 represented in Fig.1 and Equation (1and 2). In addition, the NiO/PJC composite was prepared by the above-
88 cited method without purging the air. The obtained $Ni(OH)_2$/carbon was termed as PJNH and it was
89 calcinated to convert NiO/carbon composite which was termed as PJNC. This process is also indicated in
90 Fig.1 and Equation (3 and 4).

91 **Synthesis I:**

92 $$\mathrm{PJC} + \mathrm{O_2} + \mathrm{Ni(NO_3)_2} + 2\,\mathrm{NaOH(aq)} \rightarrow \mathrm{PJC-O_2-Ni(OH)_2}\downarrow + 2\mathrm{NaNO_3(aq)} \quad \textbf{(1)}$$

$$\mathrm{PJC} - O_2 - \mathrm{Ni(OH)_2} \xrightarrow{\triangle} \mathrm{NiO} - \mathrm{PJC\ (PJGNC)} + O_2 + H_2O \qquad \textbf{(2)}$$

Synthesis II:

$$\mathrm{PJC} + \mathrm{Ni(NO_3)_2} + 2\,\mathrm{NaOH(aq)} \rightarrow \mathrm{PJC} - \mathrm{Ni(OH)_2} \downarrow + 2\mathrm{NaNO_3(aq)} \qquad \textbf{(3)}$$

$$\mathrm{PJC} - \mathrm{Ni(OH)_2} \xrightarrow{\triangle} \mathrm{NiO} - \mathrm{PJC\ (PJNC)} + H_2O \qquad \textbf{(4)}$$

2.4 Characterization

The PJGNC and PJNC morphology were uniquely distinguished by using FESEM (SUPRA 55 VP-4132 CARL ZEISS), XRD analysis (SmartLab, RIGAKU). The composition of elements presented in PJGNC and PJNC was differentiated and quantified by EDAX analysis. The variance in magnetic property between PJNOC and PJNC was meticulously studied using 7410 VSM (Lakeshore) analysis. The adsorption/desorption nitrogen isotherm in the P/P_o range at 77.3 K (ASAP 2020 V4.02 H) were utilized to accurately differentiate the specific surface area and pore size of the PJGNC and PJNC.

2.5 Batch mode adsorption studies

Using acceptable standards and methods, the comparison of removal capacity of the prepared adsorbents was analysed by batch adsorption studies. In this study, 100 mL of optimal concentrations of lead (II) ions solutions were taken with the specified amount of adsorbents in the reagent bottles. Subsequently using a mechanical shaker with 180 rpm, they were agitated at 300K to elucidate the optimal dosage of the adsorbents in the adsorption process and the optimum pH from initial concentrations of Pb(II) ions. The role of pH in the adsorption process was investigated by equilibrating 100 mLof 10 mg/L of Pb(II) ions solution with 1.0 g/L of dried adsorbents at various pH values between 1.0 and 8.0. The adsorbents ranging from 0.5g/L to 1.0 g/L were surveyed with specified Pb(II) ions solution to find their optimal dose. The probability of the adsorption process was studied. The finest pH and the composite doses were accurately determined as 6.0 and 1.0 g/L for both PJNC and PJGNC. All the batch experiments were carried out with the abovementioned parameters with an equilibration time of about 180 minutes. After each batch experiment, the supernatant solution was decanted and analysed by using atomic absorption spectrophotometer (AAS - WFX-130 - Systronics). Therefore, the amount (q_t) of Pb (II) ions adsorbed could be calculated by the following equation (5) and the adsorption efficiency (R_t) could be calculated using the equation (6):

$$\text{Amount of Pb(II) ions removal } (q_t)\ (\mathrm{mg/g}) = \frac{(C_i - C_e)\mathrm{V}}{\mathrm{W}} \qquad \textbf{(5)}$$

$$R_t = \frac{(C_i - C_e)}{C_i} \times 100\% \qquad \textbf{(6)}$$

whereC$_i$is the metal ions concentration measured before adsorption, C$_e$is the metal ions concentration measured after adsorption, W is the weight of the dried adsorbent andV is the aqueous solution volume in liter.

2.6 Isotherms analysis

The unique design of the adsorption system could be correlated by the adsorption isotherm (Hameed et.al 2008; Saravanakumar et.al 2019). It would be necessaryto explain the dispersion of adsorbate on the adsorbent in the liquid phase (Yao et.al 2016). The batch adsorption results in this present study were analysed using the two major isotherm models such as Freundlich isotherm and Langmuir isotherm. First one indicated the equilibrium distribution of Pb(II) ions between the solid and liquid phase. This isomer was valid effectively for only monolayer adsorption onto a surface with a finite quantitynumber of active sites. This isotherm model assumed unchanging/uniform energies of adsorption onto the surface and no drifting/ transmigration of adsorbate in the surface of adsorbent (Singh 1989; Bouabidi et.al 2018).Langmuir isotherm could be represented by following equation (7):

$$\text{Qe} = \frac{Q_{0.}b_L C_e}{(1+b_L C_e)} \quad \textbf{(7)}$$

Linear form of Langmuir equation (8)could be represented as,

$$\frac{C_e}{Q_e} = \frac{1}{Q_0 b_L} + \frac{C_e}{Q_0} \quad \textbf{(8)}$$

Where C$_e$is the equilibrium concentration of Pb(II) ions (mgL^{-1}), Q$_e$is the amount of Pb(II) ions adsorbed per gram of the adsorbent at equilibrium (mg/g), Q$_o$is the maximum monolayer coverage capacity (mg/g) and b$_L$is the Langmuir isotherm constant (L/mg)

The Freundlichisotherm is used to pronounce/ describe the adsorption of metal ions on the heterogeneous surface. This isotherm does not necessitate limit of the adsorption when coverage is satisfactory/sufficient to fill a monolayer. It could be represented by the following equation (9) and equation (10) (Khozhaenko et.al 2016):

$$Q_e = k_F . C_e^{1/n} \quad \textbf{(9)}$$

$$log\ Q_e = \log k_F + \frac{1}{n}\log C_e \quad \textbf{(10)}$$

where *n* is the adsorption intensity, $k_F$is theFreundlich isotherm constant (mg/g), $Q_e$is the amount of Pb (II) ions adsorbed per unit gram of the adsorbent at equilibrium (mg/g) and$C_e$is the equilibrium concentration of adsorbate (mg/L).

3. Results and discussion

3.1 Structural variation in PJNC &PJGNC

The structural variance of the PJNH and PJGNH composites could be understood by the powder-XRD pattern which is shown in Fig.2. The 2θ values of both PJNH and PJNOH are related to the respective Miller indices (001), (100), (101), (102), (110), (111) and (200)(Huang et al 2007). The broadened peak of PJGNH and PJNH indicated poor crystallinity. The intensity of PJGNH was a little higher than PJNH. It showed the orientation effect of purged gases on the precipitation of nickel hydroxide. It supported high aggregation of $Ni(OH)_2$ with an outer layer of carbon particles. The reduced intensity peaks on PJNH indicated the domination of carbon on precipitation (Poinern et.al 2009). The crystalline structure of PJNC and PJGNC could be explained by the powder XRD analysis. Fig.3 shows the powder XRD analysis of PJNC and PJGNC. The 2θ values of both PJNC and PJNOC were matching to the corresponding (111), (200), (220), (311) and (222) Miller indices (Mahmoud et.al 2015; Suresh et.al 2016; Wu and Hsieh 2008; Xiang et.al 2002). The observed values denoted the presence/existence of the nano NiOcrystalline in the composite. The peak intensity of PJGNC was higher than PJNC. It indicated the extent of crystallinity of PJGNC (Inoue and Hirasawa 2013). The sharp peaks of PJGNC specified mesopore size enlargement. It clearly supported the formation of $Ni(OH)_2$ influenced by purged air. The continued purging of air tended to disperse properly of the carbon particles in the liquid phase on precipitation of $Ni(OH)_2$. It also led to the quantized effect (Jayaram and Prasad 2009).

FTIR spectral analysis

The FTIR analysis reports of PJNC and PJGNC are indicated in Fig.4. The PJNC and PJGNC composites were derived from *prosopis juliflora*. Therefore, it showed peaks of the functional group present in PJC. In Table 1, the observed peaks and presented functional groups were represented along with the assignments (Pallarés et.al 2018;Shen et.al 2009; Saravanakumar et.al 2013; Khalil et.al 2010). The wood-derived adsorbents comprised a combination of cellulose, hemicellulose and lignin content. Hence, the composites PJNC and PJGNC showed peaks of the primary functional group of O-H at 3781 and 3785 cm^{-1} (Tang et.al 2019). The peak at 1055 cm^{-1} indicated the ester (-C–O–C-) assembly. Carbonyl stretching for acetyl C-O groups in aldehyde and hemicellulose groups of lignin was characterized by the existence of the peaks at 1691 cm^{-1}. The observed peaks at 1741, 1678 and 1067 cm^{-1} could be confirmed the occurrence of C-O, C = C and C –O–C respectively (Khalil et.al 2010). The prominent peak around 590 $cm^{-1}$was used to establish the presence of NiO group in the composites (Tang et.al 2019; Suresh et.al 2016)

Zeta potential studies

Generally,the solution pH impacts the surface charge on the adsorbent (Priya et.al 2018; Karthik et.al 2011). The point of zero charges (pH_{pzc}) of the adsorbent is one of the important factors to predict the range of pH which shows maximum adsorption (Tang et al. 2019). The pH_{pzc}can be calculated by the plot of pH Vs Zeta potential. As per Fig.5, pH_{pzc} of PJNC and PJGNC were calculated and the values arerespectively 6.0 and 5.7. It was manifest that PJNC had neutral surface charge at pH(6.0), positive (zeta potential + 23 mV to 3 mV) surface charge at pH(< 6.0). Then it showed negative (zeta potentials −5 mV to −29 mV) surface charge above the pH (> 6.0). The zeta potential style for PJGNC slightly fluctuated and differed compared to PJNC.

Similarly, PJGNC had positive surface charge (zeta potential + 19 mV to +4 mV) at pH (< 5.7), negative surface charge (zeta potentials -2 mV to −34 mV) at pH (> 5.7) and neutral surface charge at pH (5.7) (Tsuchidaet.al 1986). The pH_{pzc} of both PJNC &PJGNC was lowerthan pure NiO nanoparticles (pH_{pzc} = 10.8), which obviously confirmed that the surface of NiO was impacted by PJC(Acharya et al. 2009). The high pH_{pzc} value of PJNC had confirmed the decomposition of functional groups in the carbon of the composite andit led to the decrease of the negative sites on the adsorbents. Meanwhile, the dissolved gases present in the PJGNH were influenced to avoid the decomposition of the functional group during calcinations (Feygensonet.al 2010). It could be confirmed by the low pH_{pzc} of PJGNC. The negative (-ve) surface of PJGNC influenced the positively charged Pb(II) ions and generates the interactions among Pb(II) ions and showed higher removal efficiency than PJNC.

BET analysis and Particle size of adsorbents

The composite synthesis method resolute the surface properties of the material. The Brunauer-Emmett-Teller (BET) model precisely revealed how metal oxide had combined with PJ carbon. The mean pore diameter (d) values, total pore volume (P/P_o), and specific surface area (A_{BET}) were calculated and the values were tabulated in Table 2. This result showed that the surface area and pore volume of PJNC were lower than PJGNC. The dioxygen in PJGNHat calcination enlarged the mean pore diameter of PJGNC. The average particle sizes of PJNC and PJGNC were deliberateusing particle size analyzer (Horiba SZ100, Japan) and reported as 71±5 nm &89±5 nm respectively. Both composite particle sizes were higher than PJC (37 nm) and this confirmed the aggregation of NiO with PJC.

SEM-EDAX analysis

The scanning micrographs (FE-SEM) precisely differentiated the morphology of PJNH and PJGNH. Fig.6 (a and b) shows the aggregation of $Ni(OH)_2$ with PJC. It revealed that high accumulation of $Ni(OH)_2$

took place in PJGNH due to the accessibility of more available active sites which were influenced by the dissolved oxygen. The micrograph of Fig.6c visibly confirmed the fascinated gases between $Ni(OH)_2$ and PJC. It is purposefully/ intentionally caused to increase the surface area and pore diameter of PJGNC composite throughout the calcination process (Mahmoud et.al 2015). The micrographs Fig.6(d) and (f) indicate the structures of PJNC and PJGNC respectively. Fig.6f displays the mesoporous structure of PJGNC which was created by purged gases. The Fig.6(e) and 6(g) denote the PJNC and PJGNC after adsorption of Pb(II) ions. It reveals that the high amount of Pb (II) ions adsorbed on the surface of PJGNC was due to the influence of the high surface area, pore diameter and more active sites on the adsorbent (Tang et.al 2019).

The SEM - EDAX elemental dot maps of PJNH and PJGNH are shown in Fig. 7(a). The light green, violet and brown dots in the figure epitomize the concentrations of O, C and Ni respectively. The presence of more luminous intensity of dots indicates the significant concentration of the element (Tsuchida et.al 1986). In this mapping, the light green dots indicate that the quantity of oxygen distribution is a highly abundant in PJGNH when compared to PJNH. The EDAX analysis 7(b) and 7(c) also confirmed the presence of high quantity of dioxygen in the PJGNH.

VSM analysis

Generally, the potential removal of powder adsorbent from the effluent after treatment is remarkably difficult. It could be made easy when using magnetic adsorbent. The magnetic properties of nano composites were characterized using a VSM graph (Gupta et.al 2011). From Fig. 8, the hysteresis loop of both the adsorbents revealed an antiferromagnetic character (Tang et.al 2018). This type of small hysteresis loops are meant to be the soft type magnets and complete magnetisation enhances its low squareness shape. The magnetization value of PJGNC (87×10^{-3} emu/g) and PJNC (14×10^{-2} emu/g) were found to be decreased compared to pure NiO (65 emu/g) due to the presence of nonmagnetic carbon. It confirmed the successful composition of nonmagnetic carbon along with NiO. The value of coercivity in the composite PJGNC is 125.65 G and 113.95 G for PJNC. These low coercivity values of both the adsorbents confirmed soft magnetic nature (Feygenson et.al 2010).The very low value of retentivity also signposted/indicated that easier demagnetisation of the prepared composite (Ghaemiet.al 2010). Hence, both could act as good adsorbents in the effluent remediation field.

Reverberation of Synthesis process

Generally, the nature of the composite is influenced by the synthesis method. In this study, NiO/C composite was synthesized in two alternative ways. Initially, the carbon and $NiNO_3$ solution were purged

with air. The dioxygen present in the air was dissolved in this solution and combined on the surfaces and micropores of the carbon in the liquid phase. It is influenced to combine the Ni^{2+} ions with PJ carbon (Tsuchida and Muir 1986). After adding NaOH solution, the Ni^{2+} precipitated along with dioxygen entrapped between $Ni(OH)_2$ and carbon. The entrapped oxygen has been clearly shown in the FESEM micrographs [Fig.6(c)]. The EDAX analysis also supported the presence of high dioxygen content in PJGNH compared to PJNH by showing high luminous intensity and weight percentage of O_2. At calcination, the entrapped gases would leave in the form of CO, CO_2 and O_2. The released gases enlarged the micropores of composite to mesopores. It was confirmed by BET analysis. At the same time, it avoided the decomposition of the active functional group present in the PJ carbon. The functional group present in the PJGNC enhanced the negative surface charge on the composite, which was also confirmed by Zeta potential study.

3.2 Performance of Pb (II) removal

Effect of pH

The adsorption efficiency of the adsorbent usually depends on the pH of the solution (Gupta et.al 2011). The impact of pH on adsorption efficiency was examined between ranges of pH values from two to nine. Fig.9 clearly denotes that the removal efficiency of both adsorbents had decreased after pH 7 due to precipitation of Pb(II) ions (Tang et.al 2018). Below pH 2, PJNC and PJGNC did not perceive the significant amount of Pb(II) ions. It specified, the Pb(II) ions adsorption on adsorbent active sites entered/competed by the hydrogen (H^+) ions (Gerçel and Gerçel 2007; Ghaemiet,al 2017).On increasing the pH, the adsorption efficiency of both the adsorbents increased due to decrease of the hydrogen ion concentration. On increasing the pH from 2 to 6, the removal percentage of PJNC and PJGNC adsorbents increased from 34% to 83% and from 36% to 93% respectively. The adsorption capacity of PJNC and PJGNC attained a maximum at pH 6 due to the availability of the negative surface charge on the adsorbents. However, the efficiency of PJGNC was found to be significantly higher than PJNC due to the incidence/presence of more dynamical active sites on PJGNC.

Effect of adsorbent dosage

The impact of adsorbent dosage on the removal/confiscation of Pb (II) ions are reflected in Fig.10. It denotes that the removal efficiency of both the adsorbents had increased abruptly with the increase/intensification in the adsorbent dosage. It was found that on increasing the adsorbent dose, the number of availability of active sites also amplified. Therefore, it favorably helped to increase the adsorption efficiency (Acharya et.al 2009). While increasing the weight of adsorbents from 0.5g/L to 10.0g/L, the removal efficiency of PJNC increased from 76.69 to 95.68 %. Similarly, the removal efficiency of PJNC

improved from 73.59 to 93.58 %, 63.81 to 83.48 % and 54.86% to 79.06% for 20, 30 and 40 mg/L of Pb(II) ions concentration respectively at constant temperature (303 K) and at pH 6. Comparatively, adsorption capacity of Pb (II) on PJGNC increased from 88.12 to 98.54%, 86.34 to 97.42% 84.43 to 95.22 and 81.22% to 95.12% for10, 20, 30 and 40 mg/L of Pb(II) concentration ions respectively with the rise in the adsorbent doses from 0.5g/L to 10.0 g/L at constant temperature (303K) and at pH 6.0. Fig.10 shows that PJGNC had recorded higher adsorption efficiency due to the influence of the high surface area, pore diameter and pore volume of PJGNC (Jaiswal et.al 2015).

Effect of initial concentration

The removal efficiency of the adsorbent varied depending upon the concentrations of the adsorbate (Jaiswalet.al 2015). The effect on modification of concentration was assessed between the concentrations from 4 to 40 mg/L. These outcomes in Fig.11 (a and b) demonstrate that change in concentration of adsorbate caused a significant influence on adsorption. The Pb(II) ions removal efficiencies (mg/g) of the PJNC and PJGNC were improved when increasing the metal ions concentration, at the optimized pH and 1.0 g/L of dosage.

While accumulative the initial concentration from 4 – 40 mg/L, the adsorption capacities (mg/g) of PJNC and PJGNC were enlarged and amplified from 3.65 to 25.18 mg/g and 3.86 to 33.58 mg/g respectively. The increasing trend of both the adsorbents confirmed that the absorption of Pb (II) ions on adsorbent was simply physical adsorption. At the same time, the removal percentage of Pb(II) ions decreased with the increase in concentration (Fig. 11(a)). Thus, it showed the presence of the specific/precise limit of adsorption sites on the surface of adsorbent (Ahrouch et.al 2019; Goel et.al 2005; Khandanlou et.al 2015). The presence of more significant active sites and large pore diameter had influenced to significant increase the removal capacity of PJGNC than PJNC.

Isotherm pattern

The efficiency of adsorption is usually determined by affinity and surface properties of the adsorbents towards adsorbate. Surface nature of the adsorbent in the adsorption process could be effectively expressed by isotherm patterns (Goel et.al 2005; Mousa et.al 2016).In this study, Langmuir isotherm and Freundlich isotherm were applied to illustrate the nature of adsorption with the schematic mechanism of ions Pb(II) on PJNC and PJGNC adsorbents. The isotherm marks were derived fromFig.12 (a and b) and Fig.13 (a and b).Then, it was illustrated in Table 3. It clearly exhibited that the removal of Pb(II) ions followed the

Freundlich model more reasonably (Su et.al 2009; Shi et.al 2019). The maximum removal efficiencies of PJNC and PJGNC at 303K were 30.78 mg/g and 43.48 mg/g respectively.

The correlation coefficient (R^2) of both the isotherms existed between 0.97 and 0.99. However, the Freundlich isotherm was more fitted over the entire temperature (Yang et.al 2018).The hexagonal Pb(II) ions on adsorbents in the SEM micrograph (Fig. 6(g)) also supported the multilayer materialization/ formation. Thus, the following were demonstrated from the Freundlich isotherm:

- the multilayer exposure coverage was outward between the adsorbate and adsorbent at a persistent constant temperature(Li et.al 2018)
- 1/n value was below one (1/n < 1), which directed reversible physisorption (Dada et.al 2012)and
- The superior adsorption capacity of PJGNC was confirmed by higher K_f value.

The nature of the reactions was specified by using the R_L value which was obtained from Langmuir isotherm. It also specified the shape of the isotherm to be either irreversible ($R_L = 0$) or unfavorable ($R_L > 1$) or favorable ($0 < R_L < 1$) and linear ($R_L = 1$). In this study, R_L values were placed between $0 < R_L < 1$, which also definite that the adsorption was a favorable process (Habtegebrel and Khan 2018). Comparing the isotherms models, this collegial adsorption process involved both monolayer and multilayer adsorption with a fraction of active sites (Yang et.al 2018).These results concluded that PJGNC was a more favorable adsorbent than PNC in the removal of Pb (II) ions from the aqueous solutions.

4. Conclusions

The surface enhancement of PJNC and PJGNC composite was evidently investigated in this study. Pb(II) ions removal efficiency of adsorbents which was synthesized in the two different processes was investigated. The novel preparation of the composite gave high pore diameter, pore volume and more surface area. Additionally, carbon derived from agricultural invasive *prosopis julifora* wood was converted into cost effective nanocomposite. The XRD peak intensity revealed the extent of crystallinity and porous nature of PJGNC. At calcination of PJGNH, surface decomposition of the functional group was avoided by the presence of purged dissolved oxygen. It was visibly denoted in EDAX analysis. The anionic active –NH, C=C, –OH,C-O sites, phenolic and aromatic groups of both adsorbents were confirmed by FTIR analysis. The FESEM micrographs of PJGNH had confirmed the existence of gas molecules in between $Ni(OH)_2$ and carbon. The mesoporous nano PJGNC was evidently identified by FESEM micrographs and it also specified the addition of the more excessive amount of Pb (II) ions onto the PJGNC compared to PJNC. The mechanism of synthesis was found to prove the surface enhancement of the PJGNC. The VSM analysis also

supported the high soft magnetic character of PJGNC. The Langmuir and Freundlich isotherms were studied to investigate the surface nature of the adsorbents. The isotherm results had revealed that the maximum removal $q_e$capacity was 30.78mg/g for PJNC and 43.48 mg/g for PJGNC. The Langmuir isotherm and Freundlich isotherm equations were studied and it was found that they jointly supported the multilayer physical adsorption existing between Pb (II) ions and adsorbent. PJGNC gave high removal capacity when compared to PJNC due to the high surface area, pore diameter and pore volume. This present study revealed that PJGNC could be used to treat/delight the wastewater for the efficient removal of Pb(II) ions.

Acknowledgements

Sakthipandi is grateful to the Science and Engineering Research Board (SERB), New Delhi, India (Sanction no.: SB/FTP/PS-068/2014), for providing the financial support.

Declaration

We hereby declared that the submitted manuscript has not been published in this or in a similar form and it is not under editorial consideration elsewhere. The article is original, has been written by the stated authors who are all aware of its content and approve its submission. The authors declare no conflict of interest exists.

Availability of data

All the datasets generated during and/or analysed during the current study are available from the corresponding author on reasonable request.

Ethical approval

Not applicable.

Consent to participate

Not applicable.

Consent to publish

Not applicable

Competing Interests

The authors declare no competing interests.

Author's contribution

Saravanakumar conceptualized, wrote the paper, conducted the experimental analysis, and analyzed the findings. Muthukumar and Sivasankari compiled the literature review and wrote the paper. Sivasankari compiled the literature review and generated the graphical illustrations. Sathiyapriya wrote the theoretical

framework and the conclusion. Sakthipandi compiled the literature review and generated the graphical illustrations, interpreted the results, and compiled the data.

References

Acharya, J., Sahu, J. N., Mohanty, C. R., & Meikap, B. C. (2009). Removal of lead(II) from wastewater by activated carbon developed from Tamarind wood by zinc chloride activation. *Chemical Engineering Journal*, *149*(1–3), 249–262. https://doi.org/10.1016/j.cej.2008.10.029

Ahrouch, M., Gatica, J. M., Draoui, K., Bellido, D., & Vidal, H. (2019). Lead removal from aqueous solution by means of integral natural clays honeycomb monoliths. *Journal of Hazardous Materials*, *365*, 519–530. https://doi.org/10.1016/j.jhazmat.2018.11.037

Bouabidi, Z. B., El-Naas, M. H., Cortes, D., & McKay, G. (2018). Steel-Making dust as a potential adsorbent for the removal of lead (II) from an aqueous solution. *Chemical Engineering Journal*, *334*(Ii), 837–844. https://doi.org/10.1016/j.cej.2017.10.073

D.K, H. (1976). Review The physical properties of composite materials. *JOURNAL OF MATERIALS SCIENCE*, *11*, 2105–2141.

Dada, A.O1*, Olalekan, A.P2, Olatunya, A.M3., DADA, O. (2012). Langmuir , Freundlich , Temkin and Dubinin – Radushkevich Isotherms Studies of Equilibrium Sorption of Zn 2 + Unto Phosphoric Acid Modified Rice Husk, *3*(1), 38–45.

El-Keblawy, A., & Abdelfatah, M. A. (2014). Impacts of native and invasive exotic prosopis congeners on soil properties and associated flora in the arid united arab emirates. *Journal of Arid Environments*, *100–101*, 1–8. https://doi.org/10.1016/j.jaridenv.2013.10.001

Estela, M. C. C. B., Juliana, S., Matos, T. T. S., & Mayara, R. F. (2018). Effect of surface and porosity of biochar on water holding capacity aiming indirectly at preservation of the Amazon biome, (November 2017), 1–9. https://doi.org/10.1038/s41598-018-28794-z

Fu, W., Wang, X., & Huang, Z. (2019). Science of the Total Environment Remarkable reusability of magnetic Fe 3 O 4 -encapsulated C 3 N 3 S 3 polymer / reduced graphene oxide composite : A highly effective adsorbent for Pb and Hg ions. *Science of the Total Environment*, *659*, 895–904. https://doi.org/10.1016/j.scitotenv.2018.12.303

Gerçel, Ö., & Gerçel, H. F. (2007). Adsorption of lead(II) ions from aqueous solutions by activated carbon prepared from biomass plant material of Euphorbia rigida. *Chemical Engineering Journal*, *132*(1–3), 289–297. https://doi.org/10.1016/j.cej.2007.01.010

Ghaemi, N., Zereshki, S., & Heidari, S. (2017). Removal of lead ions from water using PES-based nanocomposite membrane incorporated with polyaniline modified GO nanoparticles: Performance optimization by central composite design. *Process Safety and Environmental Protection*, *111*, 475–490. https://doi.org/10.1016/j.psep.2017.08.011

Goel, J., Kadirvelu, K., Rajagopal, C., & Garg, V. K. (2005). Removal of lead(II) by adsorption using treated granular activated carbon: Batch and column studies. *Journal of Hazardous Materials*, *125*(1–3), 211–220. https://doi.org/10.1016/j.jhazmat.2005.05.032

Gupta, V. K., Agarwal, S., & Saleh, T. A. (2011). Synthesis and characterization of alumina-coated carbon nanotubes and their application for lead removal. *Journal of Hazardous Materials*, *185*(1), 17–23. https://doi.org/10.1016/j.jhazmat.2010.08.053

Habtegebrel, M. M., & Khan, M. A. (2018). Removal of Zn (II) and Cu (II) Ions from Aqueous Solution by Dried Prosopis JULIFLORA, *6*(1), 6–14. https://doi.org/10.11648/j.mc.20180601.12

Hameed, B. H., Tan, I. A. W., & Ahmad, A. L. (2008). Adsorption isotherm, kinetic modeling and mechanism of 2,4,6-trichlorophenol on coconut husk-based activated carbon. *Chemical Engineering Journal*, *144*(2), 235–244. https://doi.org/10.1016/j.cej.2008.01.028

Hua, M., Zhang, S., Pan, B., Zhang, W., Lv, L., & Zhang, Q. (2012). Heavy metal removal from water/wastewater by nanosized metal oxides: A review. *Journal of Hazardous Materials*, *211–212*, 317–331. https://doi.org/10.1016/j.jhazmat.2011.10.016

Huang, X. H., Tu, J. P., Zhang, C. Q., Chen, X. T., Yuan, Y. F., & Wu, H. M. (2007). Spherical NiO-C composite for anode material of lithium ion batteries, *52*, 4177–4181. https://doi.org/10.1016/j.electacta.2006.11.034

Indhu, S., & Muthukumaran, K. (2018). SC. *Biochemical Pharmacology*. https://doi.org/10.1016/j.jece.2018.04.027

Inoue, M., & Hirasawa, I. (2013). The relationship between crystal morphology and XRD peak intensity. *Journal of Crystal Growth*, *380*, 169–175. https://doi.org/10.1016/j.jcrysgro.2013.06.017

Jaiswal, A., Mani, R., Banerjee, S., Gautam, R. K., & Chattopadhyaya, M. C. (2015). Synthesis of novel nano-layered double hydroxide by urea hydrolysis method and their application in removal of chromium(VI) from aqueous solution: Kinetic, thermodynamic and equilibrium studies. *Journal of Molecular Liquids*, *202*, 52–61. https://doi.org/10.1016/j.molliq.2014.12.004

Jayaram, K., & Prasad, M. N. V. (2009). Removal of Pb(II) from aqueous solution by seed powder of Prosopis juliflora DC. *Journal of Hazardous Materials*, *169*(1–3), 991–997. https://doi.org/10.1016/j.jhazmat.2009.04.048

Khalil, H. P. S. A., Yusra, A. F. I., Bhat, A. H., & Jawaid, M. (2010). Cell wall ultrastructure , anatomy , lignin distribution , and chemical composition of Malaysian cultivated kenaf fiber, *31*, 113–121. https://doi.org/10.1016/j.indcrop.2009.09.008

Khandanlou, R., Ahmad, M. B., Masoumi, H. R. F., Shameli, K., Basri, M., & Kalantari, K. (2015). Rapid adsorption of copper(II) and lead(II) by rice straw/Fe3O4nanocomposite: Optimization, equilibrium isotherms, and adsorption kinetics study. *PLoS ONE*, *10*(3), 1–19. https://doi.org/10.1371/journal.pone.0120264

Khozhaenko, E., Kovalev, V., Podkorytova, E., & Khotimchenko, M. (2016). Science of the Total Environment Removal of the metal ions from aqueous solutions by nanoscaled low molecular pectin isolated from seagrass Phyllospadix iwatensis. *Science of the Total Environment*. https://doi.org/10.1016/j.scitotenv.2016.01.108

Kloss, S., Zehetner, F., Dellantonio, A., Hamid, R., Ottner, F., Liedtke, V., … Soja, G. (2012). Characterization of Slow Pyrolysis Biochars: Eff ects of Feedstocks and Pyrolysis Temperature on Biochar Properties. https://doi.org/10.2134/jeq2011.0070

Kosmulski, M. (2009). pH-dependent surface charging and points of zero charge. IV. Update and new approach. *Journal of Colloid and Interface Science*, *337*, 439–448. https://doi.org/10.1016/j.jcis.2009.04.072

Li, Y., Li, W., Liu, Q., Meng, H., Lu, Y., & Li, C. (2018). Alkynyl carbon materials as novel and efficient sorbents for the adsorption of mercury(II) from wastewater. *Journal of Environmental Sciences (China)*, *68*(Chunxi Li), 169–176. https://doi.org/10.1016/j.jes.2016.12.016

Luzardo, F. H. M., Velasco, F. G., Correia, I. K. S., Silva, P. M. S., & Salay, L. C. (2017). Removal of lead ions from water using a resin of mimosa tannin and carbon nanotubes. *Environmental Technology and Innovation*, *7*, 219–228. https://doi.org/10.1016/j.eti.2017.03.002

Mahmoud, A. M., Ibrahim, F. A., Shaban, S. A., & Youssef, N. A. (2015). Adsorption of heavy metal ion from aqueous solution by nickel oxide nano catalyst prepared by different methods. *Egyptian Journal of Petroleum*, *24*(1), 27–35. https://doi.org/10.1016/j.ejpe.2015.02.003

Modwi, A., Khezami, L., Taha, K., Al-Duaij, O. K., & Houas, A. (2017). Fast and high efficiency adsorption of Pb(II) ions by Cu/ZnO composite. *Materials Letters*, *195*(Ii), 41–44. https://doi.org/10.1016/j.matlet.2017.02.089

Mousa, S. M., Ammar, N. S., & Ibrahim, H. A. (2016). Removal of lead ions using hydroxyapatite nano-

material prepared from phosphogypsum waste. *Journal of Saudi Chemical Society*, *20*(3), 357–365. https://doi.org/10.1016/j.jscs.2014.12.006

Pallarés, J., González-cencerrado, A., & Arauzo, I. (2018). Biomass and Bioenergy Production and characterization of activated carbon from barley straw by physical activation with carbon dioxide and steam. *Biomass and Bioenergy*, *115*(January), 64–73. https://doi.org/10.1016/j.biombioe.2018.04.015

Poinern, G. E., Brundavanam, R. K., Mondinos, N., & Jiang, Z. T. (2009). Synthesis and characterisation of nanohydroxyapatite using an ultrasound assisted method. *Ultrasonics Sonochemistry*, *16*(4), 469–474. https://doi.org/10.1016/j.ultsonch.2009.01.007

Priya, N. S., Kamala, S. S. P., Anbarasu, V., Azhagan, S. A., & Saravanakumar, R. (2018). Characterization of CdS thin films and nanoparticles by a simple Chemical Bath Technique. *Materials Letters*, *220*, 161–164. https://doi.org/10.1016/j.matlet.2018.03.009

Saravanakumar, R., Muthukumaran, K., & Selvaraju, N. (2019). Enhanced Pb (II) ions removal by using magnetic NiO / Biochar composite Enhanced Pb (II) ions removal by using magnetic NiO / Biochar composite. *Mater. Res. Express*, *6*, 105504.

Saravanakumar, S. S., Kumaravel, A., Nagarajan, T., Sudhakar, P., & Baskaran, R. (2013). Characterization of a novel natural cellulosic fiber from Prosopis juliflora bark. *Carbohydrate Polymers*, *92*(2), 1928–1933. https://doi.org/10.1016/j.carbpol.2012.11.064

Sdiri, A., & Higashi, T. (2013). Simultaneous removal of heavy metals from aqueous solution by natural limestones. *Applied Water Science*, *3*(1), 29–39. https://doi.org/10.1007/s13201-012-0054-1

Selvaraju, G., Kartini, N., & Bakar, A. (2018). eco-friendly activated carbon from artocarpus integer bio-waste by. *Journal of the Taiwan Institute of Chemical Engineers*, *0*, 1–13. https://doi.org/10.1016/j.jtice.2018.08.011

Shackleton, R. T., Le Maitre, D. C., Van Wilgen, B. W., & Richardson, D. M. (2015). The impact of invasive alien Prosopis species (mesquite) on native plants in different environments in South Africa. *South African Journal of Botany*, *97*, 25–31. https://doi.org/10.1016/j.sajb.2014.12.008

Shaheen, S. M., Niazi, N. K., Hassan, N. E. E., Bibi, I., Wang, H., Tsang, D. C. W., … Rinklebe, J. (2018). Wood-based biochar for the removal of potentially toxic elements in water and wastewater: a critical review. *International Materials Reviews*, *0*(0), 1–32. https://doi.org/10.1080/09506608.2018.1473096

Shen, D. K., & Gu, S. (2009). Bioresource Technology The mechanism for thermal decomposition of cellulose and its main products. *Bioresource Technology*, *100*(24), 6496–6504. https://doi.org/10.1016/j.biortech.2009.06.095

Shi, Q., Terracciano, A., Zhao, Y., Wei, C., Christodoulatos, C., & Meng, X. (2019). Evaluation ofmetal oxides and activated carbon for lead removal: Kinetics, isotherms, column tests, and the role of co-existing ions. *Science of the Total Environment*, *648*, 176–183. https://doi.org/10.1016/j.scitotenv.2018.08.013

Singh, V. N. (1989). Fly-Ash for the treatment of water enriched in lead(II). *Journal of Environmental Science and Health. Part A: Environmental Science and Engineering*, *24*(7), 783–808. https://doi.org/10.1080/10934528909375516

Su, Q., Pan, B., Pan, B., Zhang, Q., Zhang, W., Lv, L., & Wang, X. (2009). Fabrication of polymer-supported nanosized hydrous manganese dioxide (HMO) for enhanced lead removal from waters. *Science of the Total Environment*, *407*, 5471–5477. https://doi.org/10.1016/j.scitotenv.2009.06.045

Sud, D., Mahajan, G., & Kaur, M. P. (2008). Agricultural waste material as potential adsorbent for sequestering heavy metal ions from aqueous solutions - A review. *Bioresource Technology*, *99*(14), 6017–6027. https://doi.org/10.1016/j.biortech.2007.11.064

Suresh, S., Jayamoorthy, K., & Karthikeyan, S. (2016). Fluorescence sensing of potential NLO material by bunsenite NiO nanoflakes : Room temperature magnetic studies. *Sensors & Actuators: B. Chemical*. https://doi.org/10.1016/j.snb.2016.03.149

Tang, N., Niu, C., Li, X., Liang, C., Guo, H., Lin, L., … Zeng, G. (2018). Efficient removal of Cd2+ and Pb2+ from aqueous solution with amino- and thiol-functionalized activated carbon: Isotherm and kinetics modeling. *Science of the Total Environment*, *635*, 1331–1344. https://doi.org/10.1016/j.scitotenv.2018.04.236

Tang, Q., Shi, C., Shi, W., Huang, X., Ye, Y., Jiang, W., … Li, D. (2019). Preferable phosphate removal by nano-La(III) hydroxides modified mesoporous rice husk biochars: Role of the host pore structure and point of zero charge. *Science of the Total Environment*, *662*, 511–520. https://doi.org/10.1016/j.scitotenv.2019.01.159

Tsuchida, N., & Muir, D. M. (1986). Potentiometric studies on the adsorption of Au(CN)2 and Ag(CN)2 onto activated carbon. *Metallurgical Transactions B*, *17*(3), 523–528. https://doi.org/10.1007/BF02670218

Wan Ngah, W. S., & Hanafiah, M. A. K. M. (2008). Removal of heavy metal ions from wastewater by chemically modified plant wastes as adsorbents: A review. *Bioresource Technology*, *99*(10), 3935–3948. https://doi.org/10.1016/j.biortech.2007.06.011

Wu, M. S., & Hsieh, H. H. (2008). Nickel oxide/hydroxide nanoplatelets synthesized by chemical precipitation for electrochemical capacitors. *Electrochimica Acta*, *53*(8), 3427–3435. https://doi.org/10.1016/j.electacta.2007.12.005

Xiang, L., Deng, X. Y., & Jin, Y. (2002). Experimental study on synthesis of NiO nano-particles. *Scripta Materialia*, *47*(4), 219–224. https://doi.org/10.1016/S1359-6462(02)00108-2

Xing, W., Li, F., Yan, Z. F., & Lu, G. Q. (2004). Synthesis and electrochemical properties of mesoporous nickel oxide. *Journal of Power Sources*, *134*(2), 324–330. https://doi.org/10.1016/j.jpowsour.2004.03.038

Yang, X., Yi, H., Tang, X., Zhao, S., Yang, Z., Ma, Y., … Cui, X. (2018). Behaviors and kinetics of toluene adsorption-desorption on activated carbons with varying pore structure. *Journal of Environmental Sciences (China)*, *67*, 104–114. https://doi.org/10.1016/j.jes.2017.06.032

Yao, S., Sun, S., Wang, S., & Shi, Z. (2016). Adsorptive removal of lead ion from aqueous solution by activated carbon/iron oxide magnetic composite. *Indian Journal of Chemical Technology*, *23*(2), 146–152.

Yuan, G. H., Jiang, Z. H., Aramata, A., & Gao, Y. Z. (2005). Electrochemical behavior of activated-carbon capacitor material loaded with nickel oxide. *Carbon*, *43*(14), 2913–2917. https://doi.org/10.1016/j.carbon.2005.06.027

Zachariades, C., Hoffmann, J. H., & Roberts, A. P. (2011). Biological Control of Mesquite (*Prosopis* Species) (Fabaceae) in South Africa. *African Entomology*, *19*(2), 402–415. https://doi.org/10.4001/003.019.0230

Zhang, X., Lin, Q., Luo, S., Ruan, K., & Peng, K. (2018). Preparation of novel oxidized mesoporous carbon with excellent adsorption performance for removal of malachite green and lead ion. *Applied Surface Science*, *442*, 322–331. https://doi.org/10.1016/j.apsusc.2018.02.148

Table 1 FTIR analysis report for PJNC and PJGNC

Position of the peak (cm^{-1})		Assignments	REF
PJNC	PJGNC		
3781	3785	O-H Stretching	Kloss et al.
3468	3458	O-H Stretching and N-H Stretching	Pallarés et al.; Jayaram et al.
3051	3051, 2923	C-H Stretching	Saravanakumar et al.; Shen et al.
2292	2337	N-H Bending	
	1741	C= O Bending	Shen et al.
1691	1678	C=C, C=O Stretching	
1463	1463	Aromatic C=C Stretching	Saravanakumar et al.
	1355	C–N peptide bond	
1194	1199	OH Bending	Khalil et al.
1068	1067	C-O-C	Jayaram et al.; Shen et al.
848	847	Aromatic =C-H out-of-plane	Pallarés et al.
591	590	NiO Stretching	Mahmoud et al.

Table 2 BET Analysis of PJNC and PJGNC

Adsorbent	PJNC	PJGNC
Specific surface area (ABET)	35 m^2 /g	58 m^2 /g
Total pore volume (P/P_o)	0.0182 cm^3 /g	0.029 cm^3 /g
Mean pore diameter (d)	1.96 nm	2.05 nm
Particle size	85 nm	94 nm

Table 3 The PJNC and PJGNC isotherm results

		PJNC			PJGNC		
		303K	313K	323K	303K	313K	323K
Langmuir isotherm	b_L (L/mg)	0.285	0.289	0.306	0.491	0.554	0.382
	q_m (mg/g)	30.769	27.712	24.631	43.478	46.083	40.984
	R^2	0.9835	0.9906	0.9892	0.9777	0.9379	0.9914
	C_o (mg/L)	R_L	R_L	R_L	R_L	R_L	R_L
	10	0.2598	0.2570	0.2463	0.169	0.153	0.208
	20	0.1493	0.1475	0.1405	0.092	0.083	0.116
	30	0.1048	0.1034	0.0982	0.064	0.057	0.080
	40	0.0807	0.0796	0.0755	0.048	0.043	0.061
Freundlich isotherm	1/n	1.890	1.978	2.092	0.5913	0.586	0.5993
	K_F (mg/g)	6.663	6.183	5.829	12.272	14.018	9.954
	R^2	0.992	0.990	0.980	0.9929	0.9955	0.9885

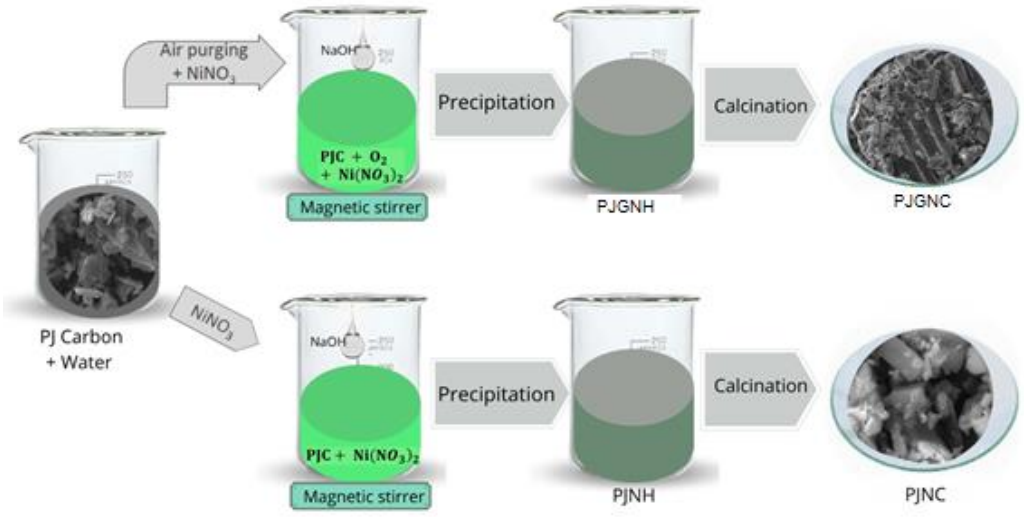

Fig. 1 Diagrammatic procedure for the synthesis of PJGNC and PJNC

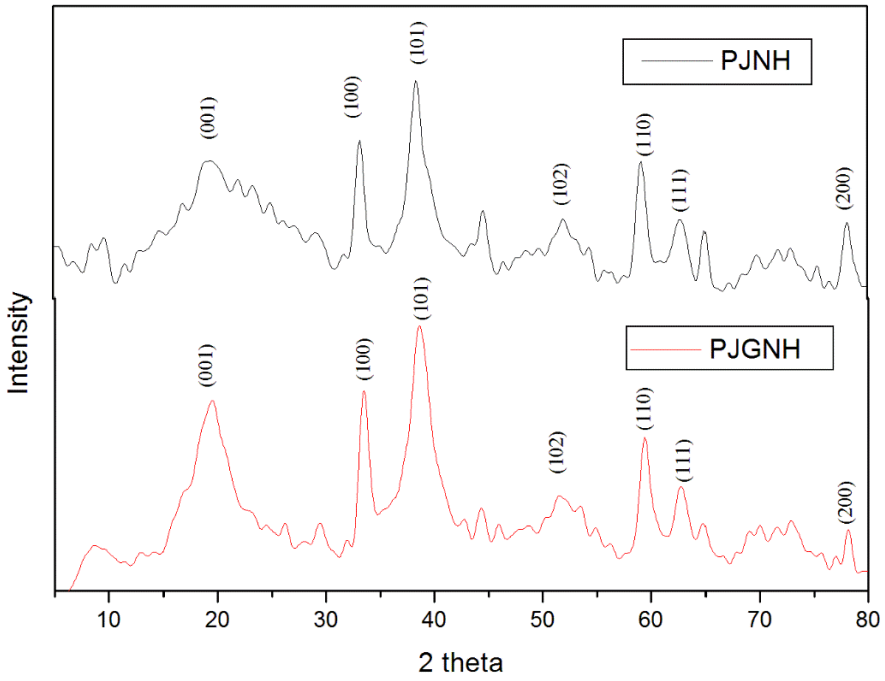

Fig.2 XRD analysis of PJNH and PJGNH

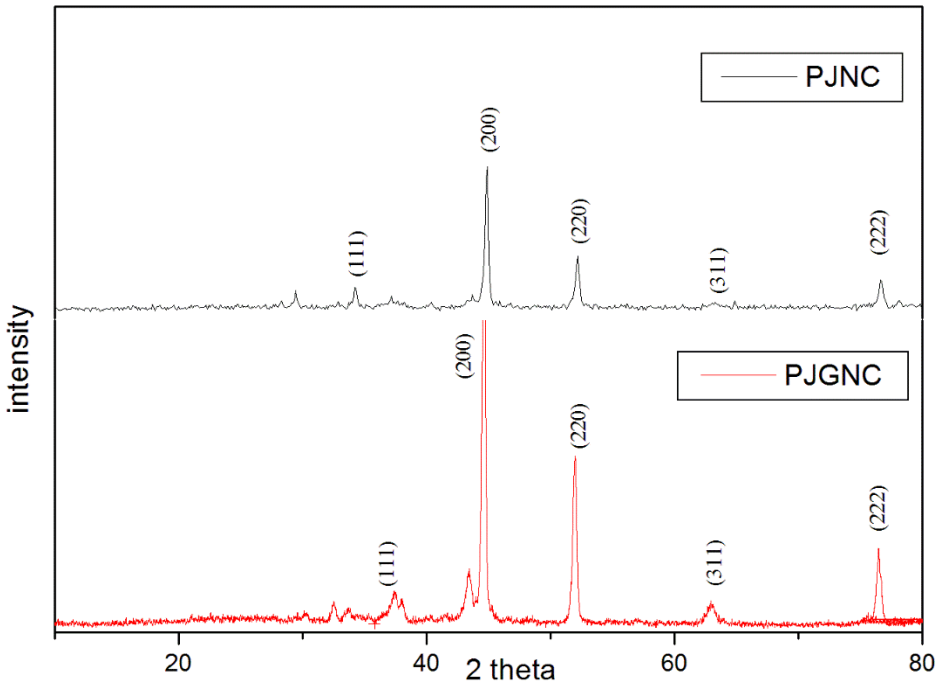

Fig. 3 XRD analysis of PJNC and PJGNC

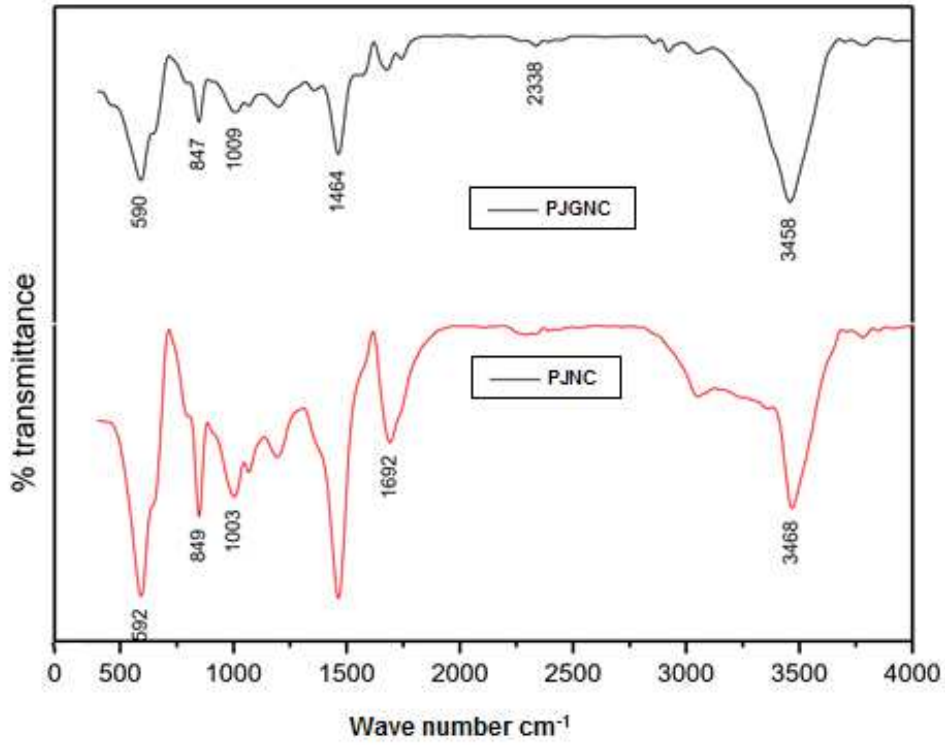

Fig. 4 FTIR analysis of PJNC and PJGNC

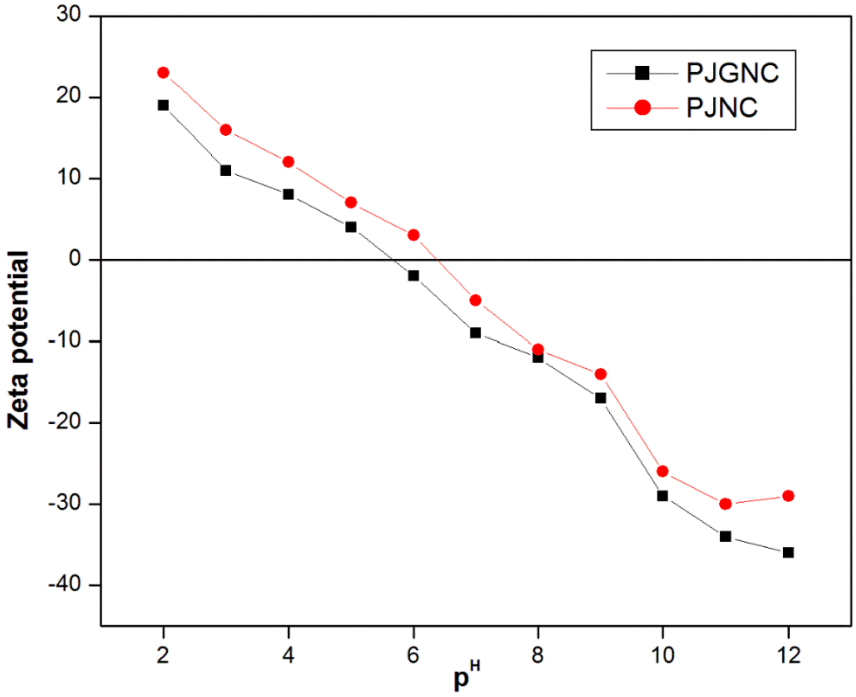

Fig. 5 pH Vs Zeta potential

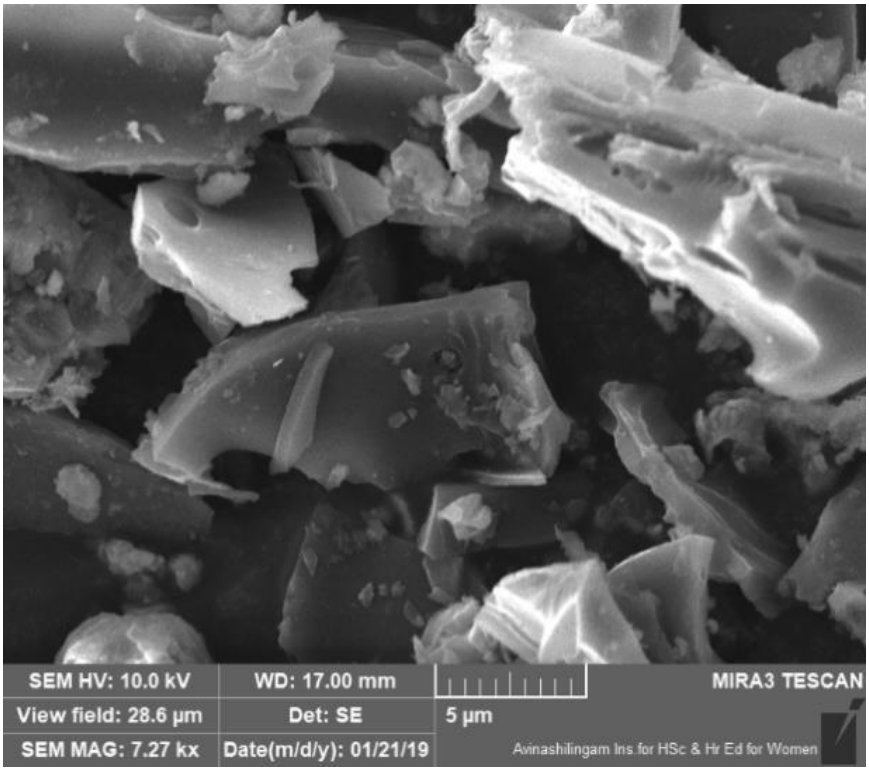

Fig. 6a SEM Image of PJNH

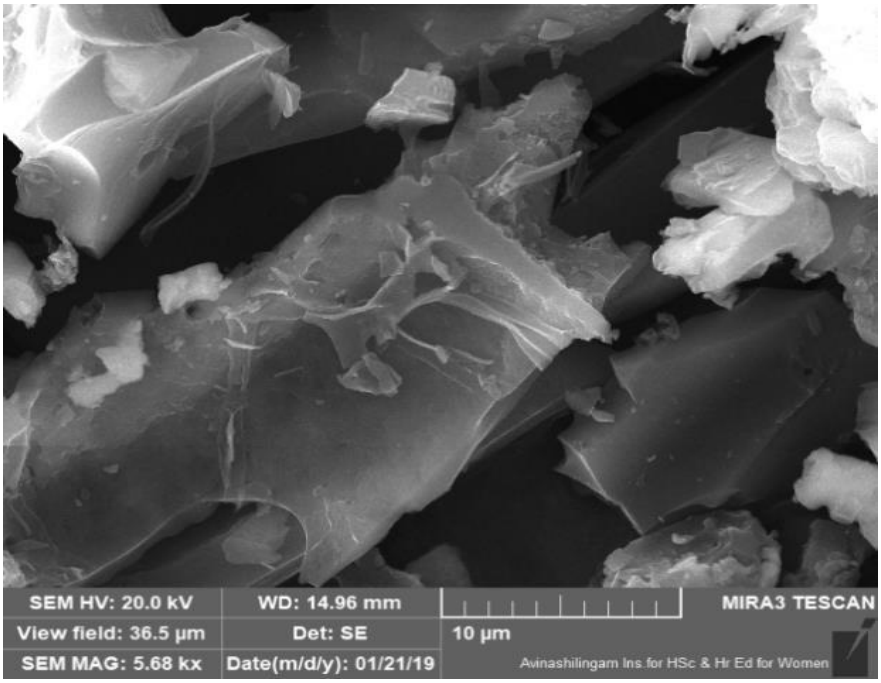

Fig. 6b SEM Image of PJGNH

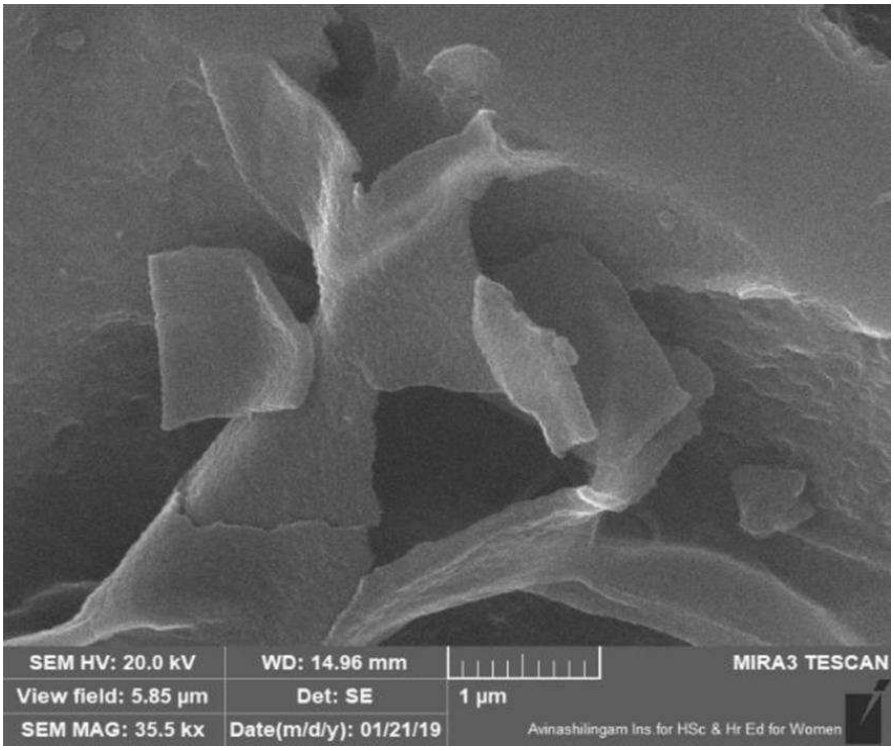

Fig. 6c SEM Image of PJGNH

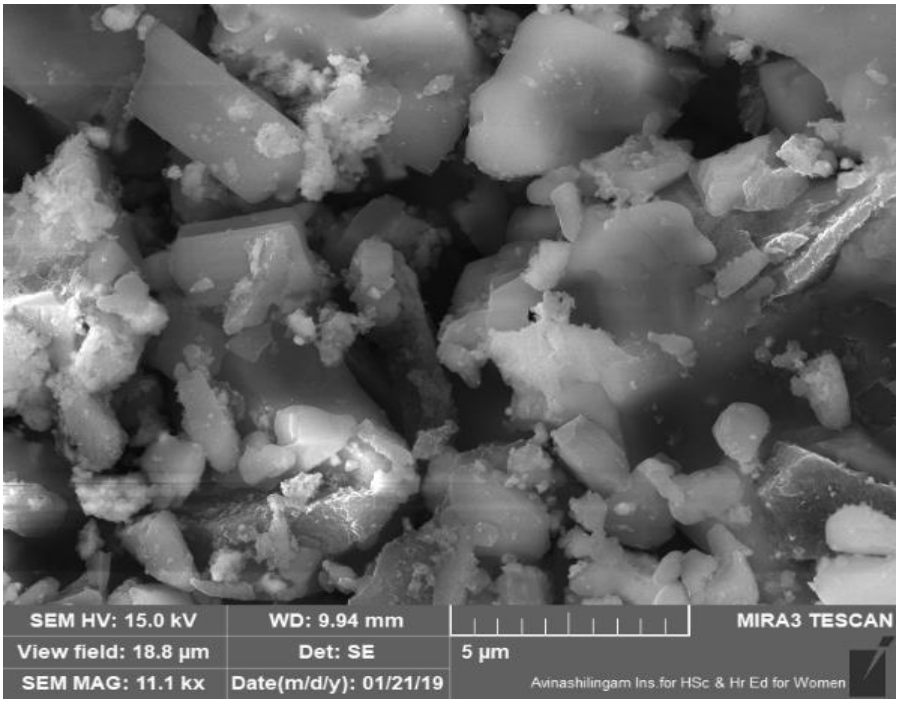

Fig. 6d SEM Image of PJNC

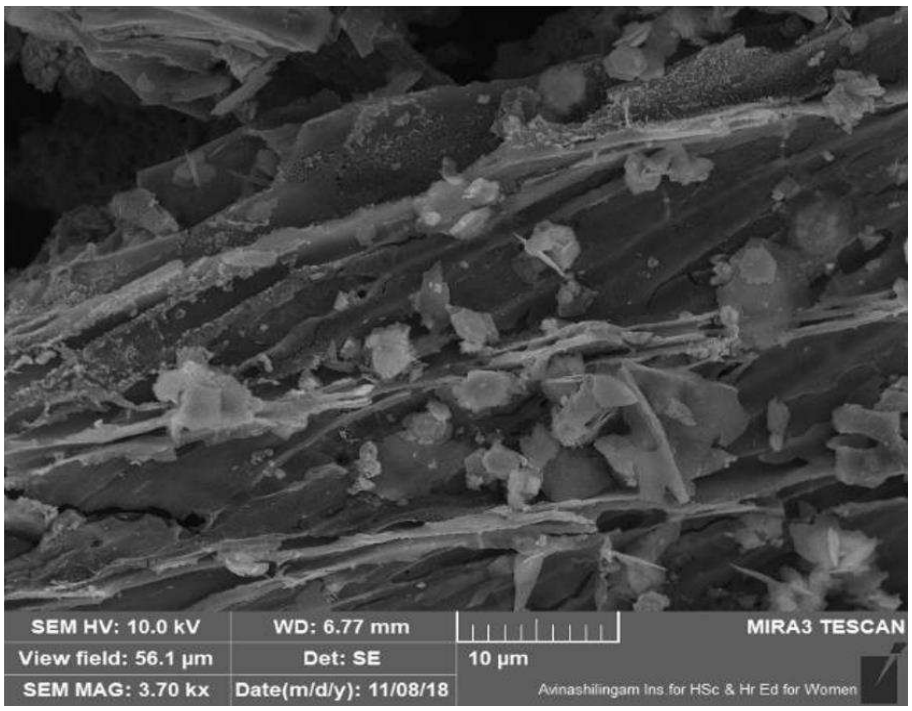

Fig. 6e SEM Image of Pb(II) loaded PJNC

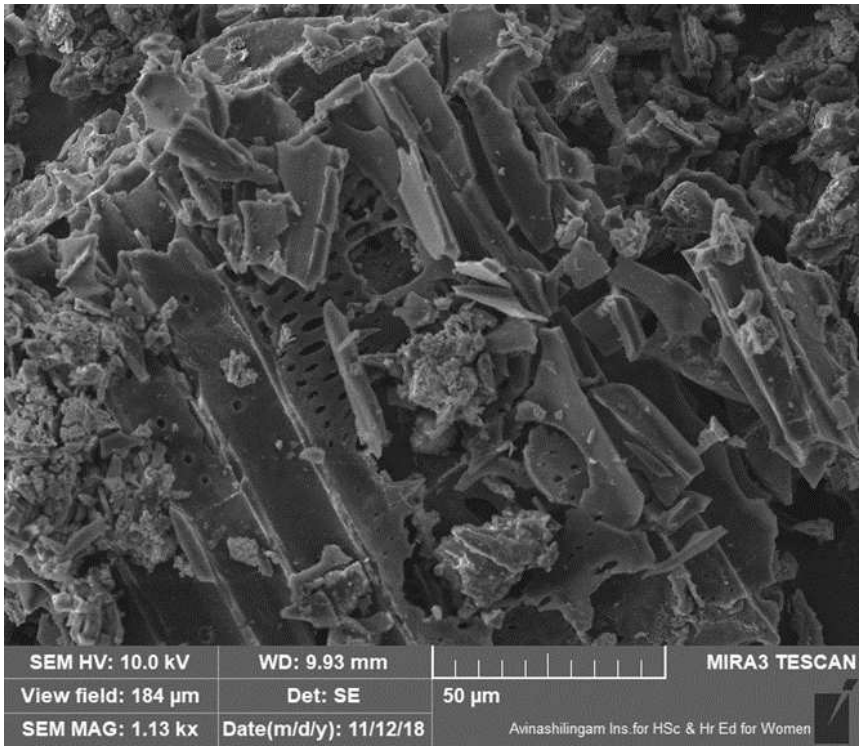

Fig. 6f SEM Image of PJGNC

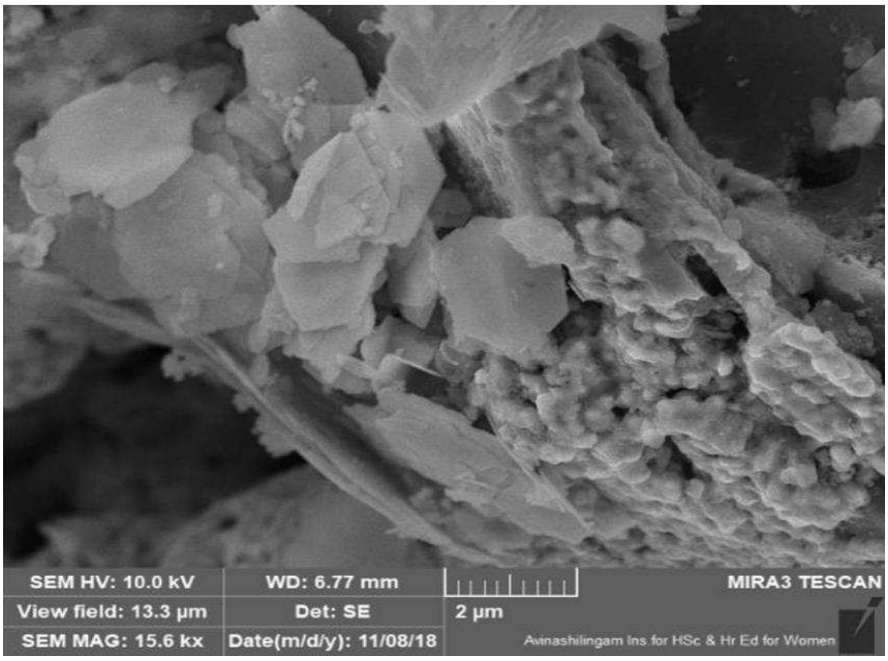

Fig. 6g SEM Image of Pb(II) loaded PJGNC

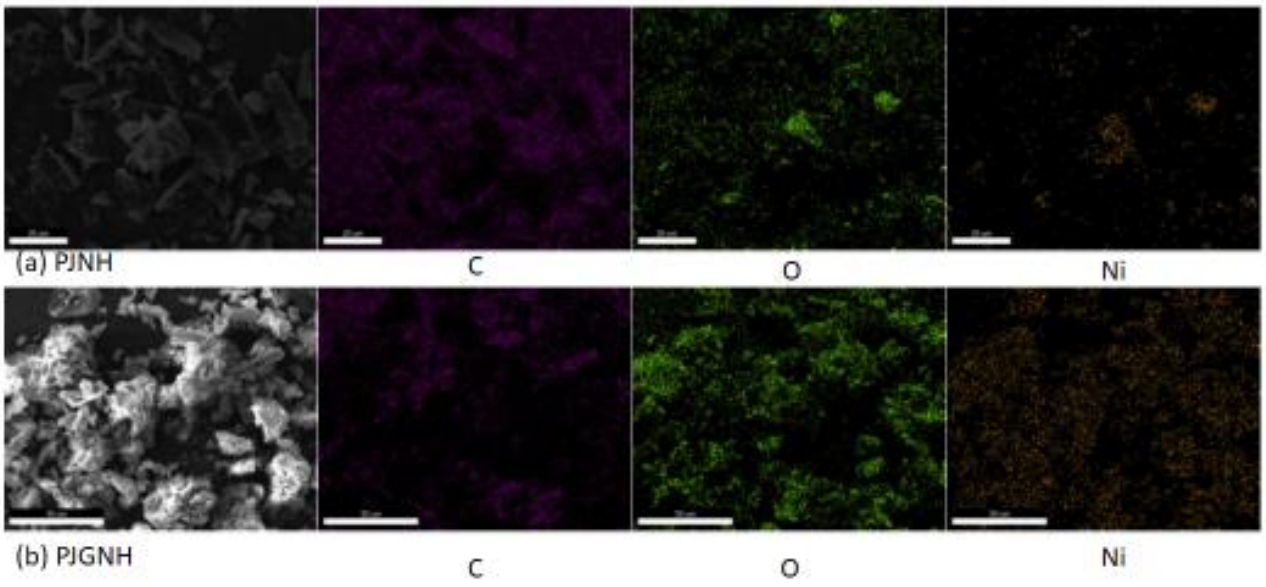

Fig. 7(a) EDAX elemental dot maps of PJNH and PJGNH

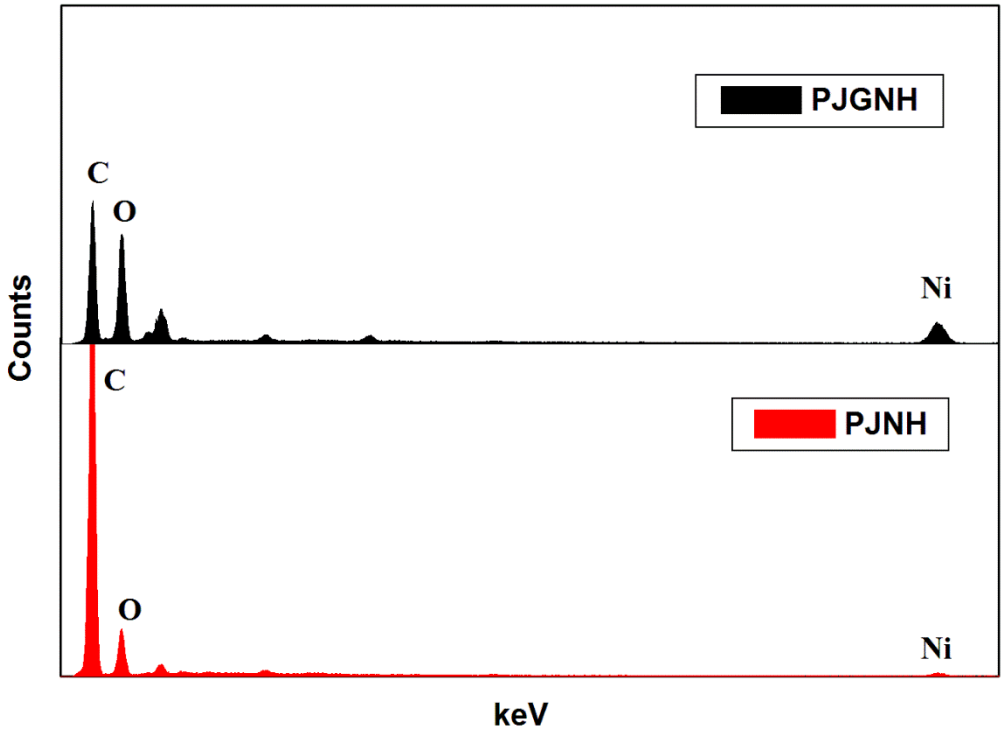

Fig.7 (b) EDAX analysis of PJNH and PJGNH

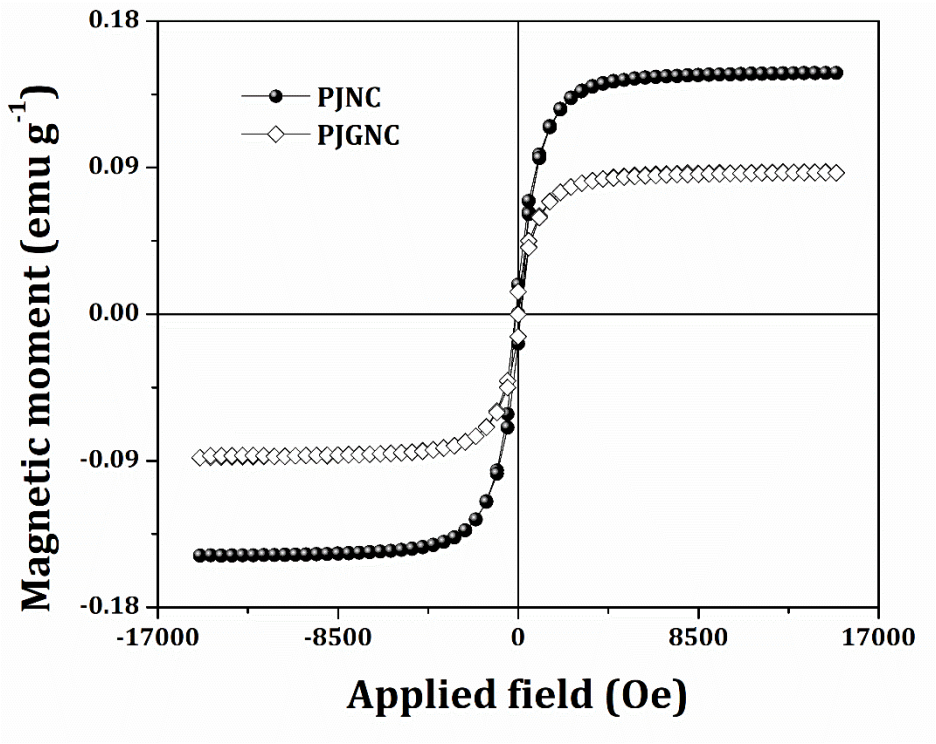

Fig. 8 VSM analysis of PJNH and PJGNH

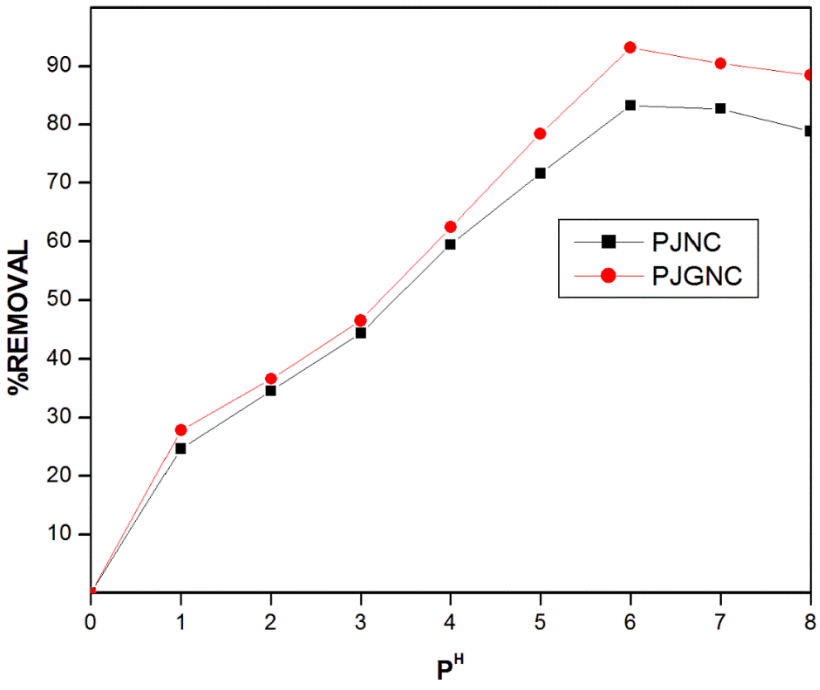

Fig.9 Effect of pH

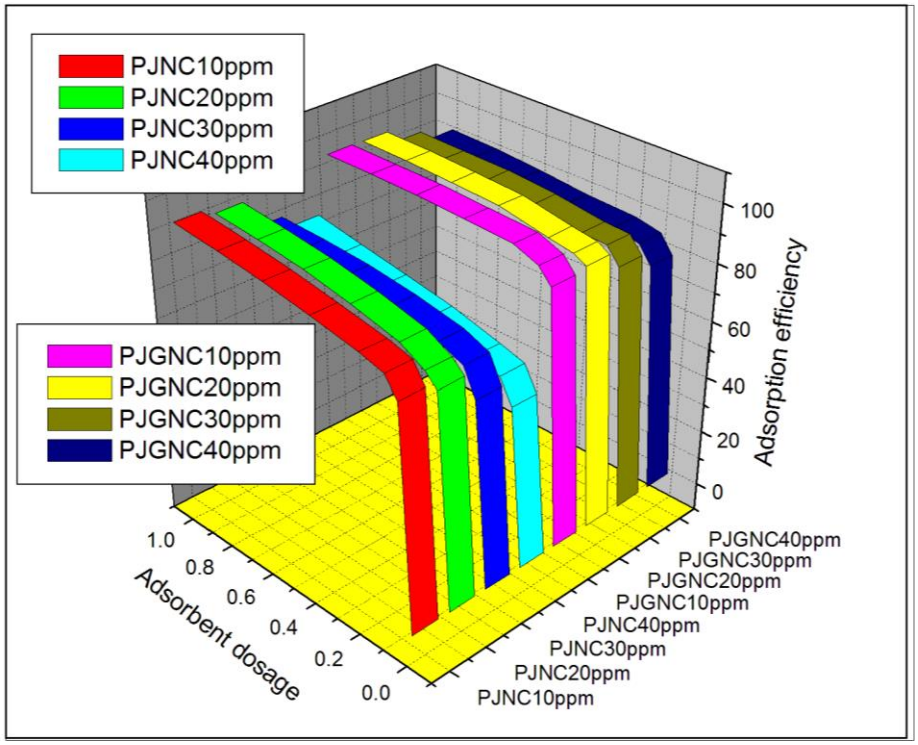

Fig. 10 Effect of adsorbent dose

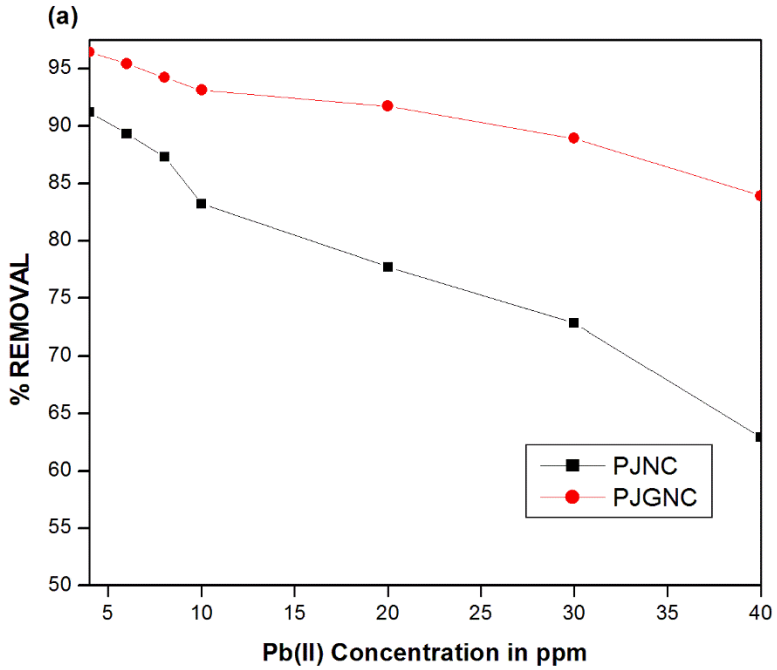

Fig. 11(a) Effect of Pb(II) ions concentration

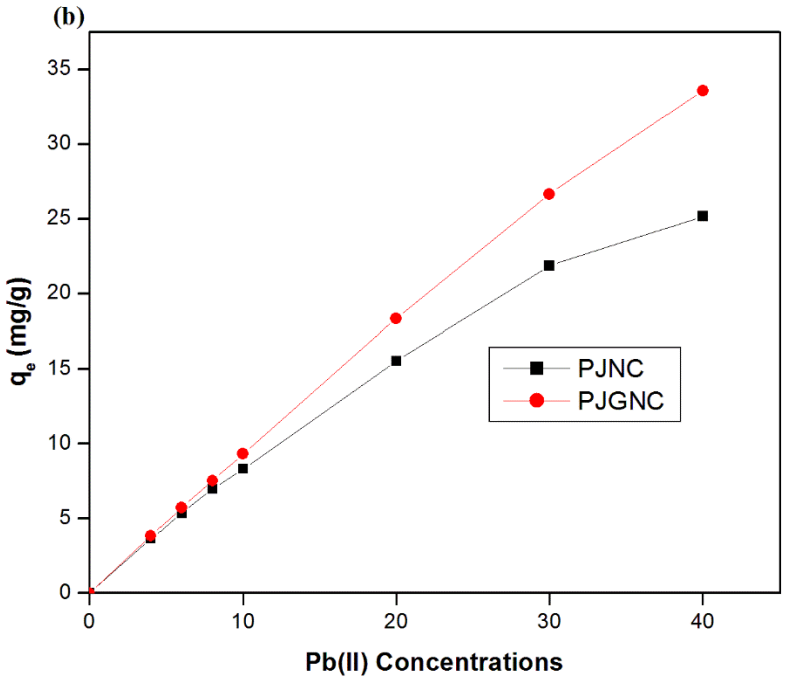

Fig. 11(b) Effect of Pb(II) ions concentration

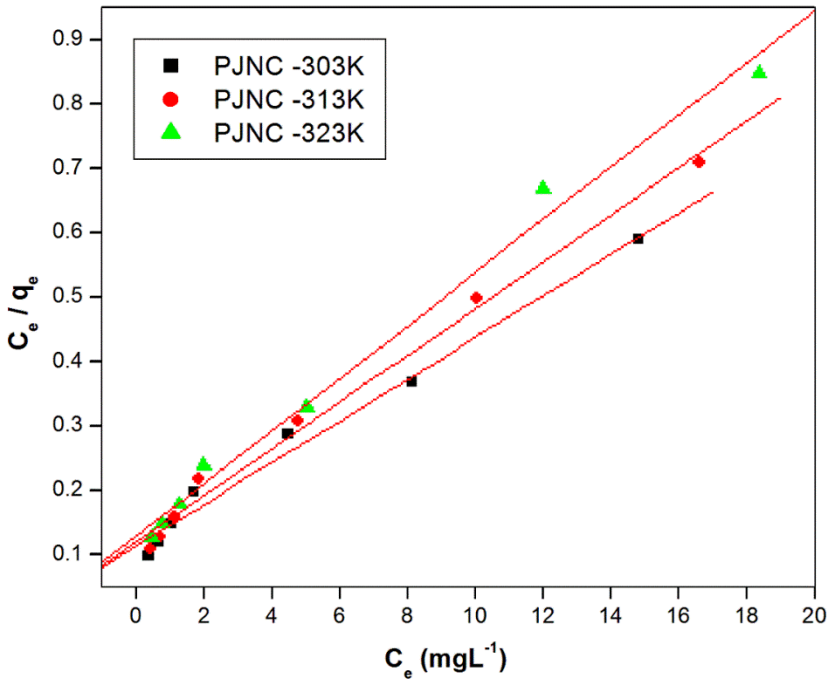

Fig.12 (a) Langmuir isotherm of PJNC

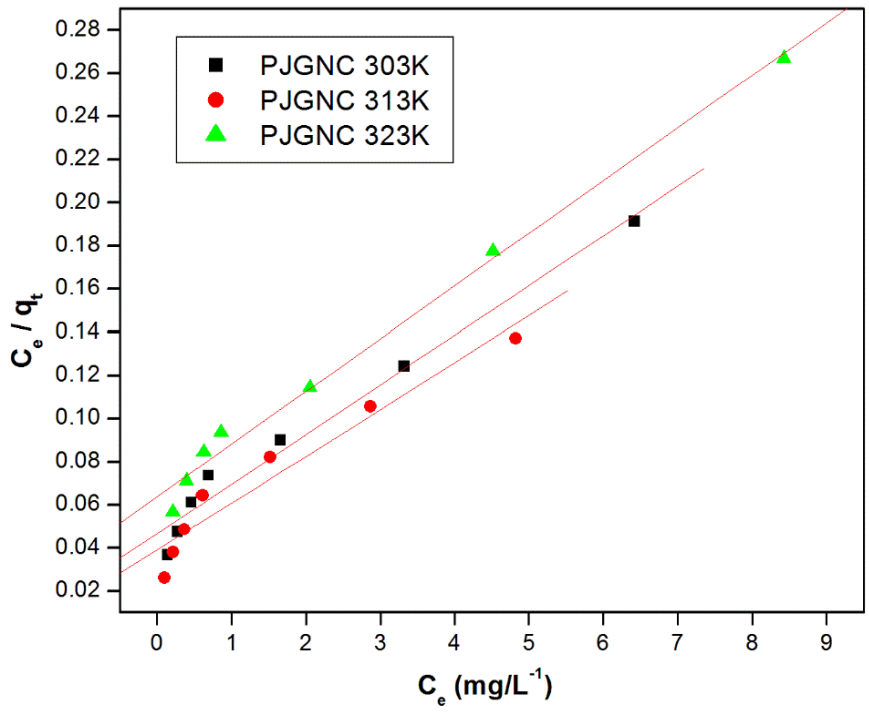

Fig. 12 (b) Langmuir isotherm of PJGNC

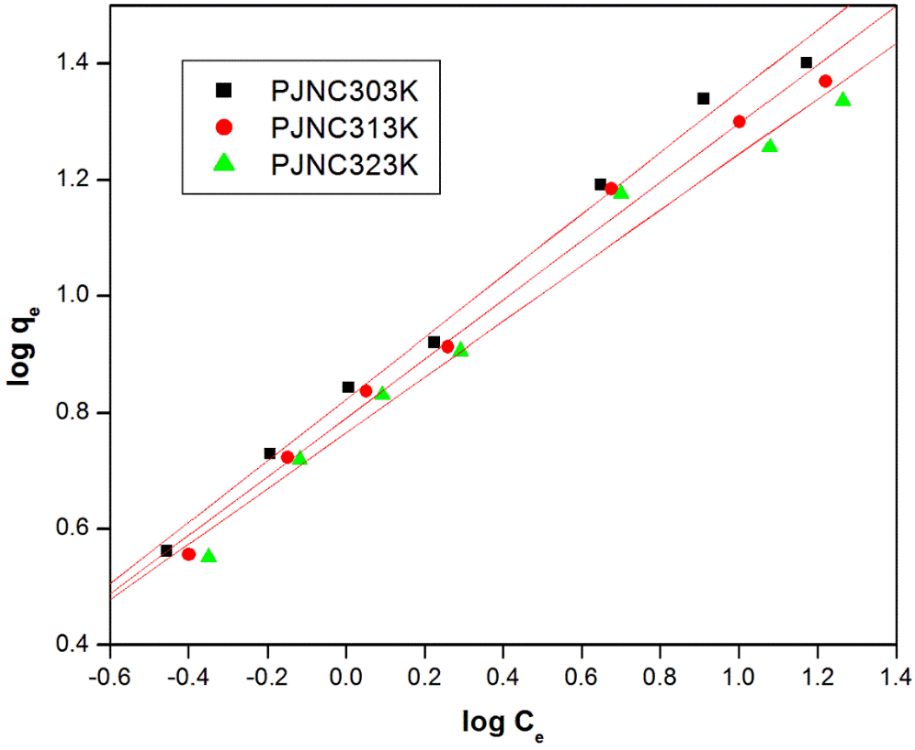

Fig. 13(a) Freundlich isotherm of PJNC

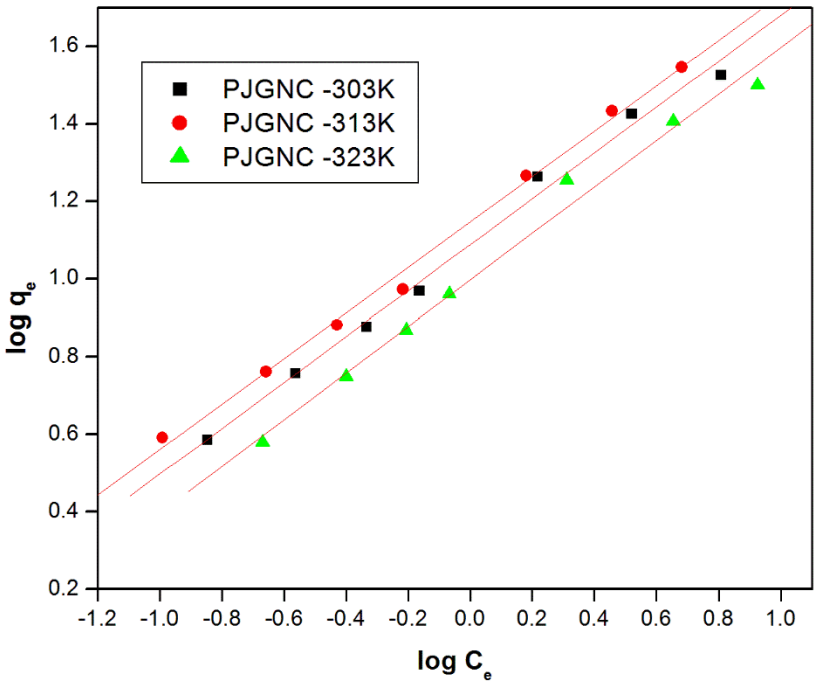

Fig. 13 (b) Freundlich isotherm of PJGNC